

Electronic supplementary material:

## Image processing

We extract the shape of the slime mould from colour photographs. The slime mould is yellow, so pixels that belong to the slime mould have a low intensity in the blue channel (we work with colour images in RGB format). Therefore this channel gives maximum contrast with the white background. We make most of our analysis on the blue channel of the images, so from now on 'image' refers to the blue channel of the image, and 'intensity' means intensity of the blue channel, unless stated otherwise. To remove fluctuations of illumination we normalize the images by dividing all pixels of each image over their average intensity. From now on we will always refer to normalized intensities (so a value of 1 corresponds to the average intensity of the image). Each photograph shows 24 dishes. We detect the centres of the dishes and their approximate radius by means of the circular Hough transform. We then use this information to cut each photograph in square pieces, each one containing one single dish. We then analyse each dish separately, and from now on we refer to the analysis of one dish.

Detecting the mould in one image is in general difficult, because of the low contrast of its branches and the inhomogeneities of the background. Instead, we detect the mould only in the first image—where it has high contrast—and from then on we detect its movement rather than the mould itself. We detect the mould in the first image by taking all pixels whose intensity is lower than 0.7, and selecting the connected component (blob) whose centroid is closest to the centre of the dish.

For each subsequent image, we monitor only those pixels in close proximity (closer than 2 pixels) to the mould's frontier. We consider that the mould has invaded one of these pixels when all of the following conditions meet: (1) The intensity of the pixel decreases with respect to its intensity in previous images, and the corresponding drop has a cumulative value higher than 0.07 (see below for the definition of cumulative value of a drop). (2) The intensity of the pixel is lower than 1.4 (this is a high threshold that we use to remove reflections). (3) The difference of the intensity (of the blue channel) minus the intensity of the red channel is lower than  $-0.07$ . We extend the mould's frontier to all pixels that meet these criteria, and check the new pixels that are now closer to the new frontier. We iterate until no more pixels are left, and then we move on to the next image of the sequence.

Cumulative value of an intensity drop: To detect and quantify significant drops in intensity for one given pixel, we proceed as follows. First we take the intensity of the pixel that occupies the same position for all images, so that we have the sequence of intensities for that position across the whole experiment. We smooth this sequence using a moving average of window 5 datapoints. Then we define a 'drop' as a period where intensity decreases monotonously over time (to allow small fluctuations, the intensity may increase once during this period). The aggregate value of the intensity drop is the difference between the intensity in the first point of the drop and the intensity in the last point of the drop. However, for a given point of the image, the background is stationary over time: If we plot the intensity of one given pixel of the background over time (i.e. for different photographs of the sequence), we find that its intensity remains roughly constant. When the mould reaches the position of this pixel, we observe a marked drop of the intensity, typically followed by a slow increase of intensity as the mould's color becomes lighter. Therefore, we characterize a pixel that is being covered by the mould by two characteristics: (1) it is adjacent to another pixel which is already covered by the mould, and (2) its intensity drops with respect to previous photographs.

To detect the drops of intensity over time reliably we first normalize each image by dividing the intensity of each pixel over the average intensity of the image, in order to control for fluctuations of illumination. Then, for each pixel, we take the sequence of its intensities over time and smooth it by means of a moving average with a window of 5 points. We then find periods where the intensity decreases monotonously. Of all these periods, we select the one where the overall decrease of intensity is largest, and record the time window in which it happens. Therefore, after this process we have a time window for each pixel of the image in which the intensity decreased most markedly.

This smoothed sequence presents a significant drop in the moment when the mould covers the pixel, but it can contain also drops in other moments, both before and after the event—especially after, because of the fluctuations in the mould's cytoplasm. It is difficult to detect the surface covered by a mould in a given image, because the contrast of the growing branches against the white background is often very weak, and irregularities of the background often have a comparable contrast. Also, while the recently formed branches usually have reasonable contrast, their colour typically softens after a few hours. However, from a sequence of images we can clearly appreciate the movement of the mould's front. Our algorithm detects this movement.

## Model appendix:

In order to find analytically the steady-states of the model (2) (with  $k = 1$  and  $\theta = 0$ ) we set  $dx_1/d\tau = 0$ ,  $dx_2/d\tau = 0$ ,  $dy_1/d\tau = 0$  and  $dy_2/d\tau = 0$  :

$$\begin{aligned}
 \phi(1 - x_1 - x_2) \frac{x_1^2 + \beta^2 y_1^2}{x_1^2 + \beta^2 y_1^2 + 1} - x_1 &= 0 \\
 \phi(1 - x_1 - x_2) \frac{x_2^2 + \beta^2 y_2^2}{x_2^2 + \beta^2 y_2^2 + 1} - x_2 &= 0 \\
 \phi(1 - y_1 - y_2) \frac{y_1^2 + \beta^2 x_1^2}{y_1^2 + \beta^2 x_1^2 + 1} - y_1 &= 0 \\
 \phi(1 - y_1 - y_2) \frac{y_2^2 + \beta^2 x_2^2}{y_2^2 + \beta^2 x_2^2 + 1} - y_2 &= 0
 \end{aligned} \tag{A.1}$$

We notice that three types of solutions are accessible straightforwardly :

1. The full homogeneous solution  $x_1 = x_2 = y_1 = y_2 = z$ .

In this case eqs. (A.1) reduce to one equation that is

$$z(\phi z(1 - 2z) - z^2 - \gamma) = 0 \tag{A.2}$$

where  $\gamma = 1/(1 + \beta^2)$ . We have therefore three solutions:

•

$$z_{s_1} = 0$$

•

$$z_{s_{2,3}} = \frac{1}{2(2\phi + 1)} \left( \phi \pm \sqrt{\phi^2 - 4\gamma(1 + 2\phi)} \right)$$

2. The case  $x_1 = y_1 = z$  and  $x_2 = y_2 = 0$  (or  $x_2 = y_2 = z$  and  $x_1 = y_1 = 0$ ).

Again, this reduces to one algebraic equation of the form

$$z(\phi z(1 - z) - z^2 - \gamma) = 0 \tag{A.3}$$

where, again,  $\gamma = 1/(1 + \beta^2)$ . This has three solutions of the form

•

$$z_{s_4} = 0$$

$$z_{s_{5,6}} = \frac{1}{2(\phi + 1)} \left( \phi \pm \sqrt{\phi^2 - 4\gamma(1 + \phi)} \right)$$

3. The case  $x_1 = y_2 = z$  and  $x_2 = y_1 = 0$  (or  $x_2 = y_1 = z$  and  $x_1 = y_2 = 0$ ).

Again, this reduces to one algebraic equation of the form

$$z(\phi z(1 - z) - z^2 - 1) = 0 \tag{A.4}$$

which have three solutions

•

$$z_{s_7} = 0$$

•

$$z_{s_{8,9}} = \frac{1}{2(\phi + 1)} \left( \phi \pm \sqrt{\phi^2 - 4(1 + \phi)} \right)$$

Out of – theoretically– 81 possible solutions (in the extreme case where  $\beta = 0$ ), we found 9 solutions which appear to be the only possible stable states. Indeed we check numerically the stability of the different branches of the figures 6 by integrating the equations (2) with initial conditions spanning all the phase space.

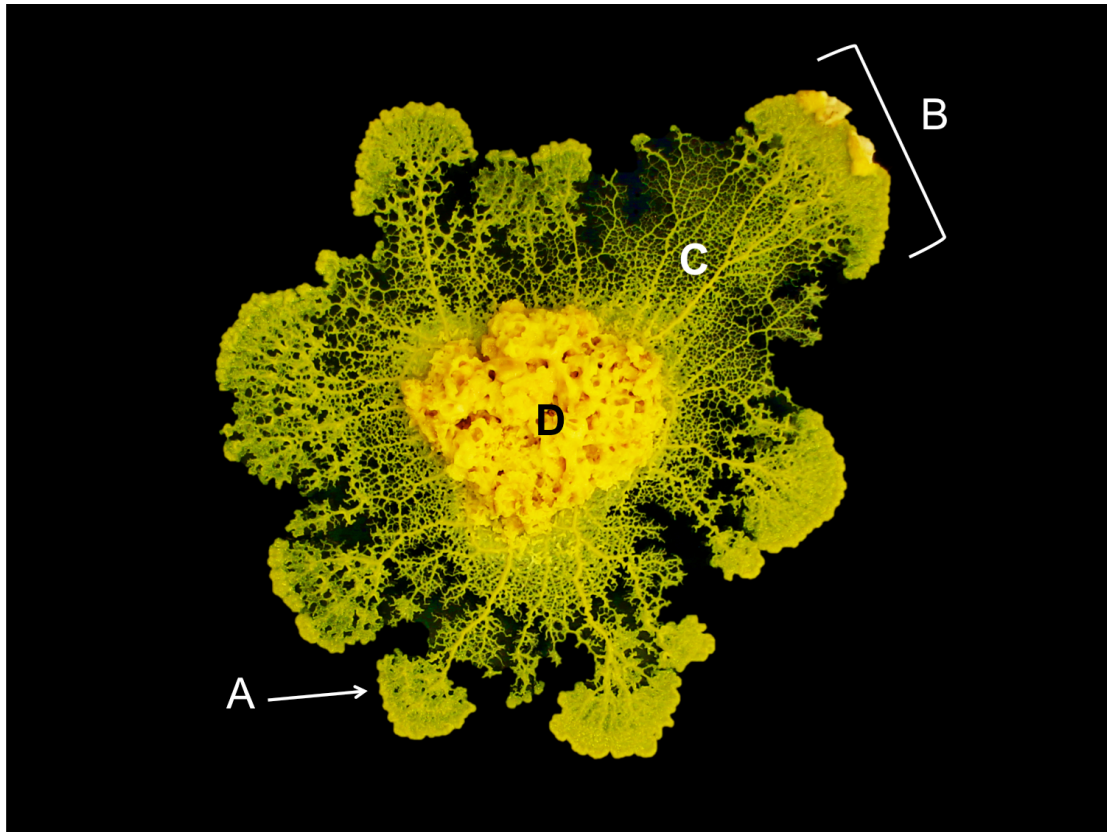


**Figure S1:** *Physarum polycephalum*. Photograph showing (A) extending pseudopod, (B) search front, (C) and tubule network. The food containing the inoculation of the cell is depicted at (D). Cytoplasm constantly and rhythmically streams back and forth through the network of tubules, enabling chemical signals and nutrients to circulate throughout the cell (c)  
Audrey Dussutour

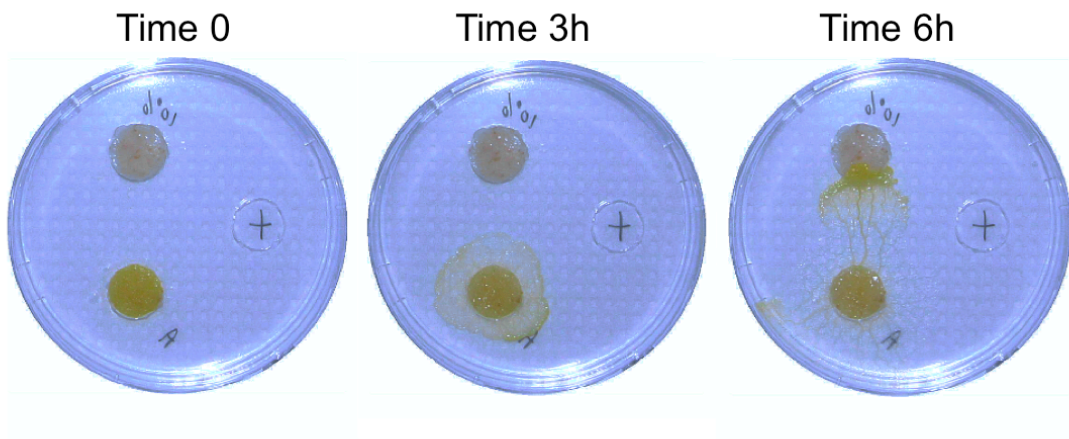


**Figure S2:** Photographs of an experiment (AG vs FD) at various times. Here the stimuli are the neutral stimulus (AG) and the food (FD). The letter A indicates that an Australian cell was monitored.

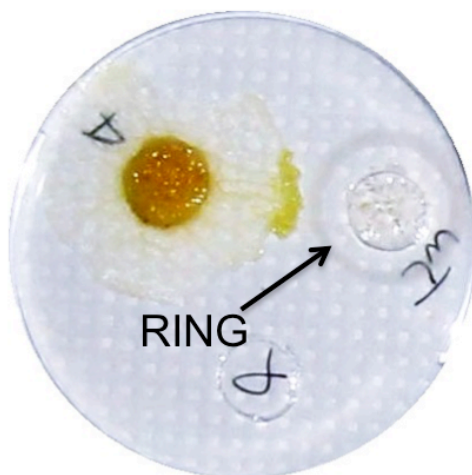


**Figure S3:** Apparition of concentric calcium precipitate rings in the agar gel during the experiment

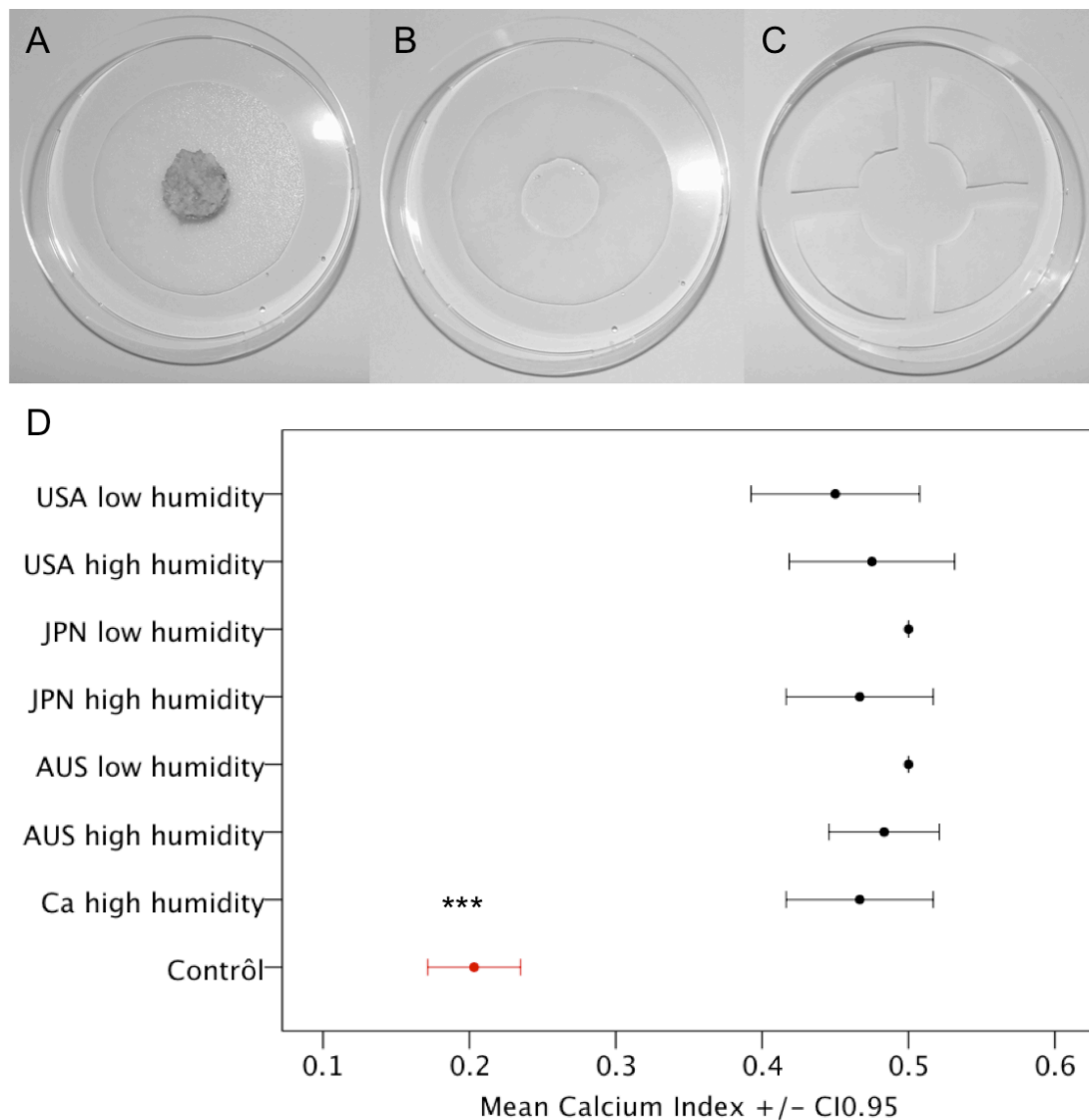


**Figure S4:** Calcium index quantified in the paper surrounding a cell and in the paper surrounding a calcium patch (0.5M CaHPO<sub>4</sub> in 1% agar). As a control we computed the calcium index in a virgin paper. The cell (or Ca patch) (diameter 18mm) was placed in the center of a humid paper (diameter 6cm, thickness 0.15mm, Grade 600, 64g.m<sup>-2</sup>) for 1h (A). We tested two level of humidity 0.1 mL of distilled water or 1mL of distilled water per piece paper. These correspond to 55% and 55% moisture level respectively. The moisture level was calculated as a percentage of the dry weight. After 1h, the cell (or Ca patch) was removed and we measured the presence of calcium in the paper. We avoided taking the paper directly in contact with the cell (or the Ca patch) by cutting a ring at 0.3cm from the cell/patch (B). To compute the calcium index, we cut the paper ring in four equal part (area 5.9cm<sup>2</sup>) and we added them one by one to a solution of solutions of Eriochrome Black T (EBT 0.05%, V=100mL) (C). EBT is a complexometric indicator that turns red when it forms a complex with calcium and magnesium. The pHs of the solutions for titration were adjusted using 0.5mL of sodium hydroxide solution (NaOH, 30%) to obtain a pH of 12. Calcium was determined at pH 12 where magnesium was precipitated as the hydroxide and did not react with EBT. Hence, the potential presence of magnesium in our stimuli did not interfere with the determination of Calcium. For each cell (or Ca patch), we recorded the number of pieces of paper added to the solution before it turned red and computed a 'calcium index' as the inverse function of the number of pieces (D). We replicated this measure 10 times for each treatment. (\*\*\*) Statistics: General linear model followed by a post-hoc test (treatment effect  $F_{1,80}=30.56$ ,  $P<0.001$ ).

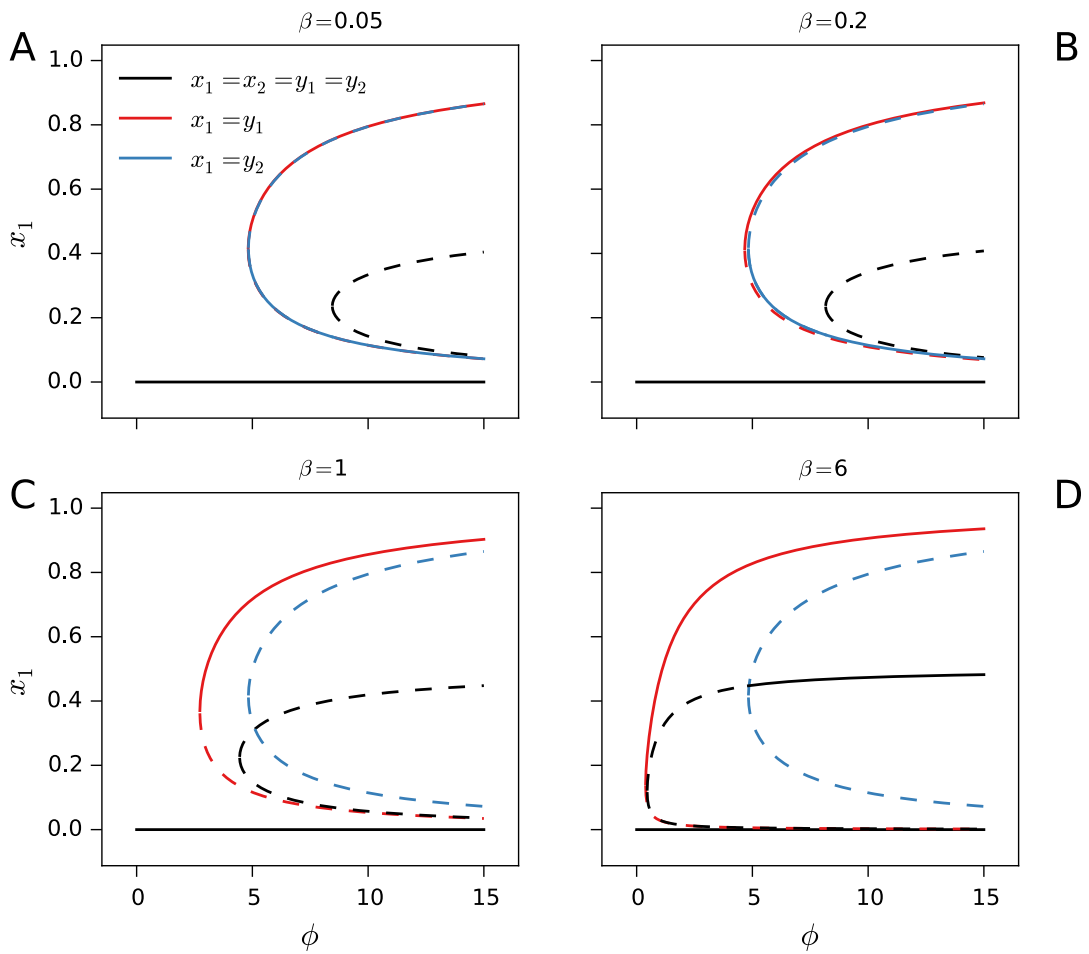


**Figure S5: Model exploration.** Bifurcation diagram of the steady states solutions of equations (2) with  $k=1$  and  $\theta=0$  as a function of the parameter  $\phi$ . Solid and dashed lines correspond to stable and unstable steady-states respectively. Parameters are  $\beta = 0.05$  (A),  $\beta = 0.2$  (B),  $\beta = 1$  (C) and  $\beta = 6$  (D). Exploring the model, we were able to make some non trivial predictions for the behavior of two cells confronted to two food sources, beyond the particular strains studied here, the key parameters (bifurcating parameters) being the speed  $\phi$  and the attraction toward a congener  $\beta$ . For small values of  $\beta$  (Figs. S3A), starting from a critical value of  $\phi$ , the branches corresponding to the selection of a same source ( $x_1 = y_1$ ) and a different food source by the two cells ( $x_1 = y_2$ ) exist and are very close. For larger  $\beta$  (Fig. S3B), the distance between the  $x_1 = y_1$  and  $x_1 = y_2$  branches starts to be appreciable (signaling a region of the parameter  $\phi$  where the solution  $x_1 = y_1$  exists while the other solution  $x_1 = y_2$  is not yet available). Increasing  $\beta$  further, results in the loss of stability of the branch  $x_1 = y_2$  and the only non-trivial solution that exists is  $x_1 = y_1$  (Fig. S3C). Finally, for larger  $\beta$  (Fig. S3D), the solution  $x_1 = y_2$  is no more stable but instead after a critical value of  $\phi$  the upper branch of the homogeneous state ( $x_1 = x_2 = y_1 = y_2$ ) becomes stable, signaling a coexistence between the latter and  $x_1 = y_1$ .

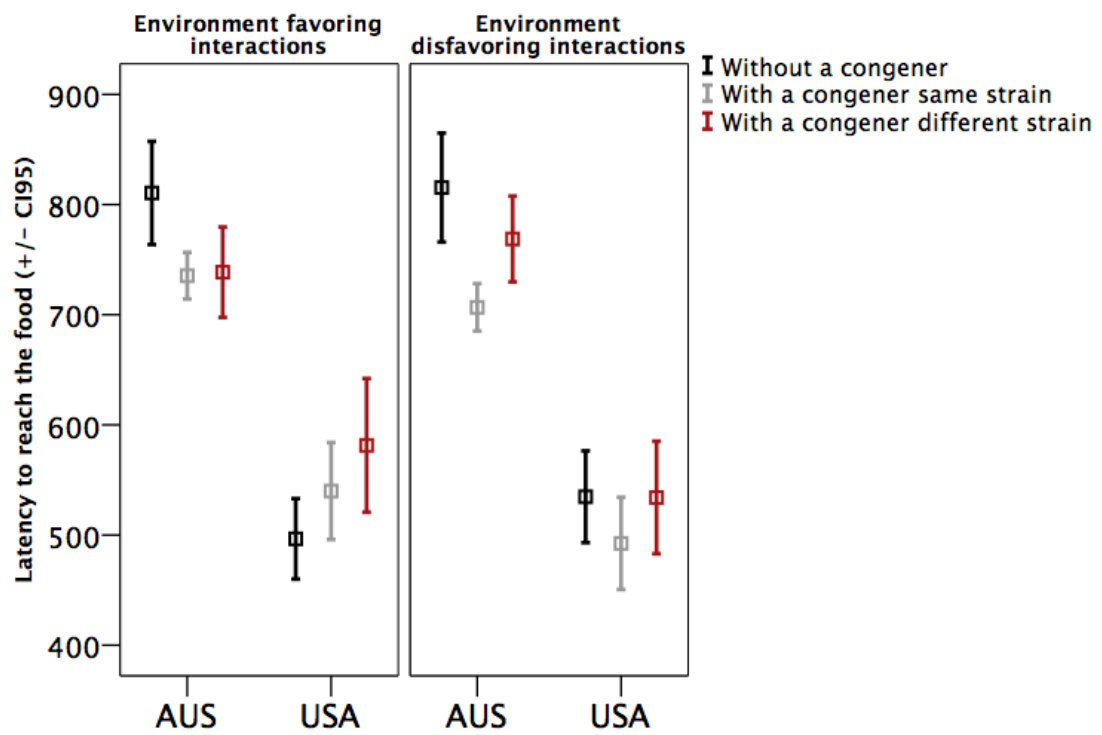


**Figure S6:** Latency to reach the food for a cell placed with a congener (same strain or different strain) and for cells on their own.